Predicting the Thermal Conductivity and Temperature Distribution in Aligned Fiber Composites

C. R. Havis,* G. P. Peterson,† and L. S. Fletcher‡
Texas A&M University, College Station, Texas

A numerical model capable of calculating the effective thermal conductivity and temperature distribution in aligned fiber composites, where the ratio of the fiber to matrix conductivities is an order of magnitude greater than unity, was developed. To determine the validity of this model, an experimental investigation was conducted utilizing cylindrical samples whose fiber direction relative to the cylinder axis varied from 0 deg to 90 deg in 15 deg increments. The temperatures, as predicted by the numerical model, were within five to eight percent of the experimentally measured values for all cases considered. Comparison of sample geometry and effective thermal conductivity indicated that the numerical model more accurately predicted the temperature distribution in samples whose fiber angle with respect to the cylinder axis was large and that accurate prediction of the edge effects, particularly in corner regions where these effects dominate, would require a three-dimensional numerical model.

Nomenclature

A	= area, m^2
A_r	= aspect ratio, $\Delta x/\Delta y$
D	= width of the modeled region, m
k	= thermal conductivity, W/m-K
k_e, k_{eff}	= effective thermal conductivity, W/m-K
k_f	= thermal conductivity of the fiber material, W/m-K
k_1,k_m,k_n	= primary thermal conductivities, W/m-K
k_{ref},k_{ss}	= thermal conductivity of the reference specimen
k_s	= thermal conductivity of the source or sink, W/m-K
k_{xx},k_{xy},k_{yy}	= thermal conductivity tensor components
n	= number of observations in a given sample, number of nodes in the sample width
q''	= heat flux, W/m^2
T	= absolute temperature, K
x,y,z	= Cartesian coordinates relative to the sample boundaries
Δ	= designates a difference when used as a prefix
δ	= designates an uncertainty when used as a prefix
v	= volume fraction
ϕ	= fiber angle

Introduction

THE use of fiber-reinforced composite materials in engineering applications has grown at an almost exponential rate over the past 20 years. Because of their high strength-to-weight ratio and dimensional stability, fiber-reinforced materials have replaced metals for applications in the aircraft, automobile, boating, chemical, electronic, and sporting goods industries.

In the manufacture of composite parts, the use of preimpregnated composite tape gives the designer the ability to specify parts of complex geometry with strengths tailored to the direction and type of loading. A typical manufacturing process consists of a mold or tool covered with this preimpregnated tape and then cured in an autoclave. To prevent thermal distortion and warping during curing, the mold must have the same thermal expansion characteristics as the composite material.

One solution to this problem is to make the molds and parts out of the same type of composite material. Recent attempts at composite mold construction appear promising, but the thermal anisotropy of the composite mold, coupled with current mold building techniques, have resulted in difficulties in attaining a uniform cure of the composite parts.[1]

For this reason, it is necessary to make accurate predictions about the thermal behavior of these materials for first-order input in transient analysis[2-4] and for composite material production. To do this, a combined numerical and experimental investigation was conducted on aligned fiber composite materials in which the fiber conductivity was an order of magnitude greater than that of the matrix material and having a volume fraction of 60%. The objective of the investigation was to determine the effects of fiber angle on the effective thermal conductivity and two-dimensional temperature distribution in these aligned fiber composites.

Analysis

There are three principal conductivities in an aligned fiber composite material: the conductivity parallel to the fibers, k_1, and the two conductivities normal to the fiber direction, k_m in the laminate plane, and k_n normal to the laminate plane. Simple analytical models used to predict the effective thermal conductivity of aligned-fiber composites consider the effect of the conductivity of the fiber and matrix material, and the fiber volume fraction, but neglect the effects of fiber orientation with respect to the heat flow and the edge effects caused by the position of the fibers relative to the sample surfaces.[5] In these models the fiber and matrix materials are assumed to behave as two resistances in parallel when the heat flow is along the fibers and in series when the heat flow is across the fibers. In addition to these simplistic models, numerous other analytical and experimental investigations have addressed the effective thermal conductivity of aligned fiber composites from a microscopic perspective with heat flow either along[6,7] or across the fibers.[8-11] Of interest here, however, is the macro-

Received April 25, 1988; presented as Paper 88-2658 at the AIAA Thermophysics, Plasmadynamics, and Lasers Conference, San Antonio, TX, June 27-29, 1988; revision received Nov. 11, 1988.

*Graduate Student, Department of Mechanical Engineering.
†Associate Professor of Mechanical Engineering. Senior Member AIAA.
‡Thomas A. Dietz Professor of Mechanical Engineering. Fellow AIAA.

scopic case in which it is necessary to predict the overall effective thermal conductivity and temperature distribution, particularly when the heat flow is at some angle to the fiber direction other than 0 deg or 90 deg. For this type of geometry, no data and only limited predictive techniques are currently available.[12]

The problem was formulated under the following set of assumptions:

1) The sample was treated as a continuum. — Since the thermocouple bead diameter was approximately 1 mm and the fiber diameter less than 10 μm, it was reasonable to assume that the effects of individual fibers were insignificant.

2) Conductivity was a function of direction. — Since the thermal conductivity of the fibers was much greater than the matrix material, the composite material was considered anisotropic.

3) Conductivity was not a function of position. — Since the composite layers were uniform throughout the sample, the material was treated as homogeneous.

4) Conductivity was not a function of temperature. — Since the thermal conductivity of the individual components, fiber and matrix materials were not significantly dependent on temperature, it was assumed that the combined thermal conductivity was not temperature dependent.

5) The heat transfer was two-dimensional. — Due to the symmetry of the sample, the fiber plane passing through the centerline was considered to be insulated.

6) The temperature distribution was two-dimensional. — Since no heat is passing through the plane being modeled, the temperature distribution in the modeled plane should be equivalent to that of any plane parallel to the modeled plane.

7) The thermal conductivity both along and perpendicular to the fibers is known. — This thermal conductivity can be found either experimentally or using one of the previously referenced techniques.

Performing an energy balance on a unit cell yields the governing equation[13]

$$k_{xx}\frac{\partial^2 T}{\partial x^2}+2k_{xz}\frac{\partial^2 T}{\partial x\,\partial z}+k_{zz}\frac{\partial^2 T}{\partial z^2}=0 \qquad (1)$$

Numerical Model

The objective of the numerical model was to solve the governing equation in a discrete region representative of a fibrous composite material. The regions modeled, as shown in Fig. 1, were the centerline cross sections of composite samples in the plane formed by the intersection of the fibers and the cylinder axis, the x-z plane. Because the property variations were planar in nature and more easily described in Cartesian coordinates, a Cartesian coordinate system was adopted.

The boundary conditions used in the formulation of the numerical model along with the domain are illustrated in Fig.

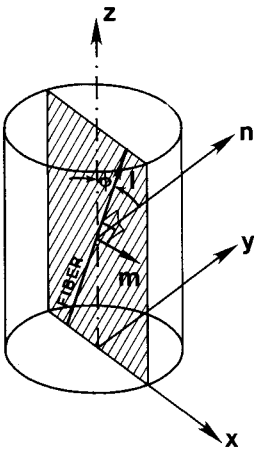

Fig. 1 Fiber direction and coordinate system.

2. The boundary conditions can be summarized as follows:

1) The sides are perfectly insulated.

2) The outer surfaces of the heat source and heat sink are isothermal.

3) There is no thermal contact resistance between the sample surfaces and the heat source and heat sink.

The approximations of the derivatives necessary to solve the governing equation at coordinates ($x=i$, $z=j$) for the temperature T_j^i were found using a finite differencing technique. The finite difference form of the governing equation is

$$\frac{k_{xx}}{\Delta x^2}(T_j^{i+1}+T_j^{i-1}-2T_j^i)+\frac{k_{xz}}{2\,\Delta x\,\Delta z}(T_{j+1}^{i+1}+T_{j-1}^{i-1}-T_{j+1}^{i-1}-T_{j-1}^{i+1})+\frac{k_{zz}}{\Delta z^2}(T_{j+1}^{i}+T_{j-1}^{i}-2T_j^i)=0 \qquad (2)$$

where

$$k_{xx}=k_1\sin^2\phi+k_m\cos^2\phi$$

$$k_{xz}=(k_1-k_m)\sin\phi\cos\phi$$

$$k_{zz}=k_1\cos^2\phi+k_m\sin^2\phi$$

The left and right boundaries were handled with the use of fictitious nodes which fit the boundary conditions. The boundary temperatures were then calculated. The phantom node temperatures T^0 and T^{n+1} were calculated from an energy balance at the boundary. For the left insulated boundary an energy balance on the surface produced

$$(T_j^0)=(T_j^{i+1})+\frac{k_{xz}}{k_{xx}}A_r(T_{j+1}^i-T_{j-1}^i) \qquad (3)$$

where Δx and Δz are eliminated by nondimensionalizing,

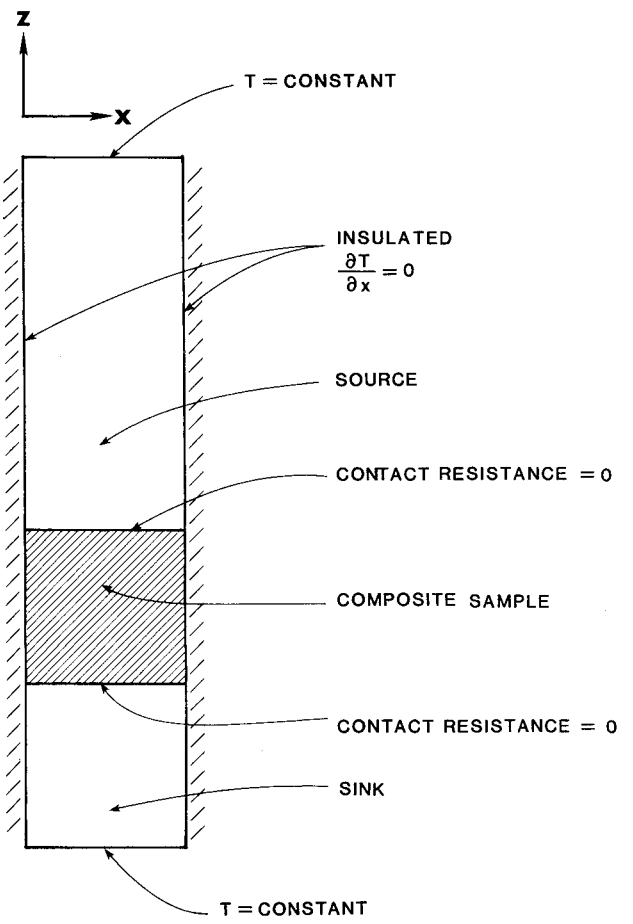

Fig. 2 Boundary conditions and domain.

using A_r, the aspect ratio defined as $\Delta x/\Delta z$. Similarly for the right boundary the phantom temperature became

$$(T_j^{n+1}) = (T_j^{i-1}) - \frac{k_{xz}}{k_{xx}} A_r (T_{j+1}^i - T_{j-1}^i) \quad (4)$$

where n is the number of nodes in the sample width, i is the x direction index, and j is the z direction index.

The upper and lower sample surface temperatures were calculated from an energy balance on those interfaces and solved for T_j^i to yield the finite difference formula for the interface temperature

$$T_j^i = \frac{k_s(T_{j+1}^i) + k_{zz}(T_{j-1}^i)}{k_s + k_{zz}} - \frac{k_{xz}(T_j^{i+1} + T_j^{i-1})}{2A_r(k_s + k_{zz})} \quad (5)$$

Upon completion of the model development, the system was solved for fiber angles of both 45 deg and 30 deg using a 17×17 grid in the sample space. This was followed by solution using a 33×33 grid. Although no significant change was observed, the 33×33 grid provided smoother temperature distribution plots and was used for all of the results presented.

Figure 3 presents temperature distributions for fiber angles from 0 deg to 90 deg in 15 deg increments. The first section, Fig. 3a, represents a 0 deg fiber angle. Here the heat is flowing parallel to the fibers. As shown in the figure, the temperature distribution is one-dimensional, with several isotherms in the reference specimen, indicating a relatively high heat transfer rate. Figure 3b shows the temperature distribution for a 15 deg fiber angle. In this figure, the temperature distribution in the central region of the sample is one-dimensional. In the regions making a 15 deg angle to the sides, indicating the areas where the fibers touch one end and one insulated side, the temperature gradient in the x and z directions is much greater at the insulated end of the fibers. A two-dimensional temperature distribution is also forming in the reference specimen near the sample interface. In the 30 deg sample, Fig. 3c, the region of the greatest temperature gradient in the x direction is again in the region where the fibers intersect one end, and one insulated side. The central region also displays a gradient in the x direction, possibly due to a constriction resistance in the reference specimen, as indicated by the large temperature gradient in the x direction, or possibly due to heat flow from the sides of the sample. Figure 3d, the 45 deg sample, shows a smoother temperature gradient in the x direction, which is to be expected since there are no continuous fibers to carry the bulk of the heat transfer and cause flat regions in the temperature profile in the central region of the sample. There does, however, appear to be more heat transfer taking place in the fibers that are nearest to being continuous, as indicated by the constriction resistance in the reference specimen. The 60 deg sample, Fig. 3e, shows the straight isotherms at even spacings in the region of fibers intersecting insulated walls on both sides. This indicates that the heat flow is one-dimensional only in the z direction. The temperature distribution is two-dimensional, because the cross conductivity induces a temperature gradient in the x direction caused by a heat flow in the z direction. For the 75 deg sample, Fig. 3f, the temperature distribution is similar to that of the 60 deg specimen, with straighter, more defined isotherms. The heat flow is also diminished, as indicated by the lack of a temperature distribution in the reference specimen. In Fig. 3g, the 90 deg sample, the temperature distribution is again one-dimensional, as was the case in the 0 deg sample.

Experimental Investigation

The objective of the experimental program was to investigate the effects of fiber direction on the heat transfer and temperature distribution of an aligned fiber composite material and to provide data for verifying the numerical model described previously.

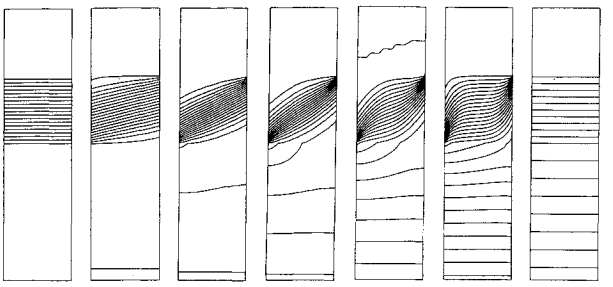

Fig. 3 Sample section profiles (0 deg through 90 deg).

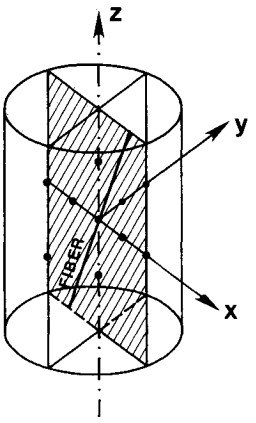

Fig. 4 Thermocouple locations.

The seven samples tested were 2.54 cm diameter cylinders, 2.54 cm long machined out of unidirectional aligned-fiber composite material. The material used was Hercules AS4/3502 prepreg tape, a graphite fiber composite, which had PAN Type II fibers in a Fibrite resin matrix with volume fraction $v = 60\%$, and a ply thickness of 12.7 μm. The test samples were constructed so that the fiber angle ϕ, as shown in Fig. 4, varied from 0 deg to 90 deg in 15 deg increments between samples. The samples were drilled (Number 56 Drill) for a total of 10 thermocouples as shown in Fig. 4. Seven thermocouples were placed in the x-z plane, 2 (one on each side) on the surfaces at the midplane, 3 on the cylinder axis at 6.35 mm, sample center, and 19.05 mm, and 2 at the midplane halfway between the center and the outer surface. Three thermocouples were placed off center on the y axis, one on each surface, and the third halfway between the sample centerline and the surface at $y = 6.35$ mm.

Test Facility

The test facility was a cut-bar apparatus, which has been described previously.[14] The device consisted of four subsystems, including a vacuum system, a test section, a thermal control system, and a temperature measurement system.

The test section consisted of a reference fixture, the test specimen, and a copper slug. The reference fixture was a 10.16 cm long by 2.54 cm diam, AISI-304 stainless steel rod. Four thermocouple holes were drilled in the reference specimen; the first was 12.7 mm from the sample interface, the next three were drilled on a 9.53-mm spacing. The copper slug was a 2.54-cm-diam copper rod with a taper machined in one end to fit the cooling plate. Dow Corning 340 heat sink compound was applied to the contacting surfaces of the sample, reference specimen, and copper slug prior to assembly to reduce the thermal contact resistance at the interface.

The thermal control system consisted of a heat source, a heat sink, and a radiation shield. The heat source was a 150 W band heater located on the upper portion of the reference specimen. The heat sink consisted of the copper slug placed in a tapered hole in an aluminum cooling plate. A constant

temperature circulating bath with a water-glycol solution removed heat from the cooling plate. The mean specimen temperature was controlled by adjusting the input heat flux (the power to the resistance heater) and the temperature of the circulating bath.

An active radiation shield was used to eliminate radiation heat transfer at the surface of the sample stack. The radiation shield consisted of an 18-cm-long by 13-cm-diam, AISI-304 stainless steel cylinder with one end embedded in the cooling plate, and a band heater around the other end. The power was controlled with a power supply similar to the one used on the heat source.

Once the test section was placed in the test fixture, and the thermocouples had all been calibrated, the test specimen was placed in the vacuum chamber. The objective of testing in a vacuum environment was to eliminate convective heat transfer from the surface of the test section. The vacuum chamber consisted of a steel cylinder 30.5 cm in diameter, with a steel plate welded on one end, and the other end tapered to fit an O-ring grove in the baseplate. The base was sealed with a Neoprene O-ring, and Dow Corning 111 compound in the groove to ensure a good seal. The vacuum was provided by a vacuum pump capable of maintaining a vessel pressure of less than 0.5 Torr. The vacuum was measured using a thermocouple vacuum gage located at the apparatus base, and monitored by a digital gage controller.

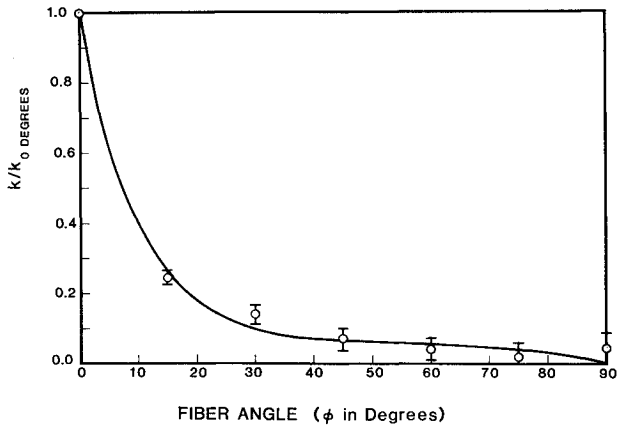

Fig. 5 Effect of variations in fiber angle on the effective conductivity.

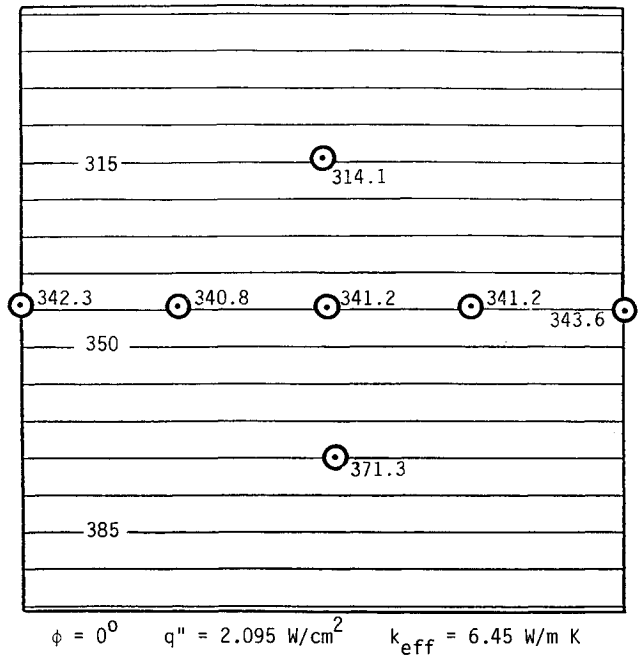

Fig. 6 Predicted two-dimensional temperature distribution.

The temperature measurement system consisted of the thermocouples, which were read by a data acquisition unit interfaced with a computer. This was the most important system in the test facility, since the temperature was the only changing variable that was measured in this system. The thermocouples used were beaded junction type K 30-AWG. Thermocouples were placed on the radiation shield, in the heat source, and in the specimen. The thermocouples exited the vessel through a vacuum feedthrough and were connected to a computerized data acquisition unit.

Experimental Procedure

The experimental procedure followed in this investigation was to place the test specimen in the test apparatus, align the test section, and apply an axial load on the vertical stack formed by the fixture, specimen, and copper slug to reduce the interfacial contact conductance. The thermocouples were connected, and the chamber evacuated. The sample heater was initially set to 12.5 W. This power input was low enough to prevent the sample from exceeding the materials maximum allowable temperature. Due to the high uncertainty in the heat flux calculation for low heat fluxes, it was important to maintain maximum temperature drop across all samples for all mean sample temperatures. Hence, the circulator bath controller was set at a temperature low enough to keep it at full refrigeration capacity, giving the maximum possible temperature drop across the specimen. The radiation heater was set to a power level that would maintain a temperature at the position corresponding to the sample midplane, which was equal to the center sample thermocouple reading.

Steady-state temperature data were recorded and used to calculate the heat flux in the sample heater, and the effective thermal conductivity of the composite sample. The system was allowed to reach steady state, defined as the condition where no thermocouple exhibited a temperature change of more than 0.5°K over a 1-h period. This usually required approximately 8 h between readings. Once the system had achieved steady state, data were recorded, the sample heater power input was incremented by 5 W, and the radiation shield heater power was increased by an appropriate amount. This was repeated until the bottom reference specimen thermocouple attained a maximum temperature of 500°K. Power to the heaters was turned off, and the system was allowed to cool before changing samples. The process was continued until all seven of the samples (fiber angles from 0 deg to 90 deg in 15 deg increments) had been tested.

The heat flow through the reference specimen was calculated as

$$q_{ss} = -k_{ss} A \frac{\partial T}{\partial z} \tag{6}$$

where A was the cross-sectional area of the reference specimen and sample and k_{ss} was the thermal conductivity of the reference specimen. The temperature gradient $\partial T/\partial z$ for both the reference specimen and the sample were calculated[15] from

$$\frac{\partial T}{\partial z} = \frac{\sum_{i=1}^{n} T_i z_i - \left(\sum_{i=1}^{n} T_i \sum_{i=1}^{n} z_i\right)\Big/ n}{\sum_{i=1}^{n} z_i^2 - \left(\sum_{i=1}^{n} z_i\right)^2 \Big/ n} \tag{7}$$

The effective thermal conductivity of the sample, k_{eff}, was calculated and by substitution of Eq. (6) for q_{ss} simplified to

$$k_{\text{eff}} = k_{ss} \frac{\partial T_{ss}/\partial z}{\partial T_{\text{samp}}/\partial z} \tag{8}$$

The results of the experimental investigation are presented in several ways. Figure 5 illustrates the effect of variations in

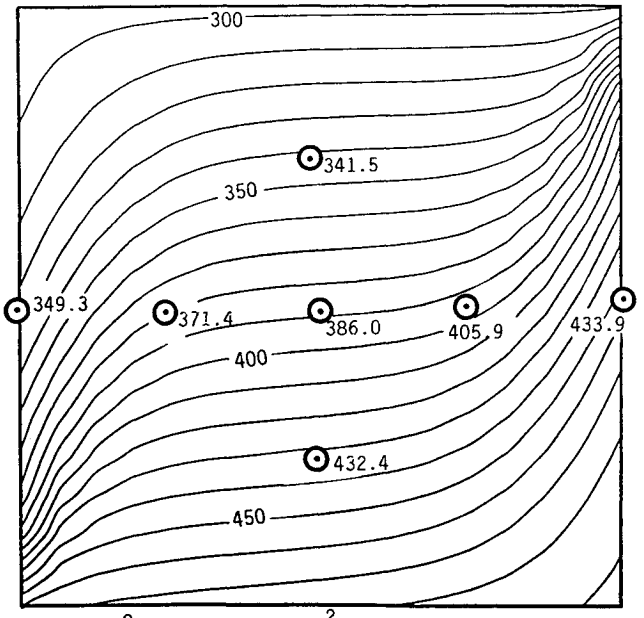

Fig. 7 Predicted two-dimensional temperature distribution.

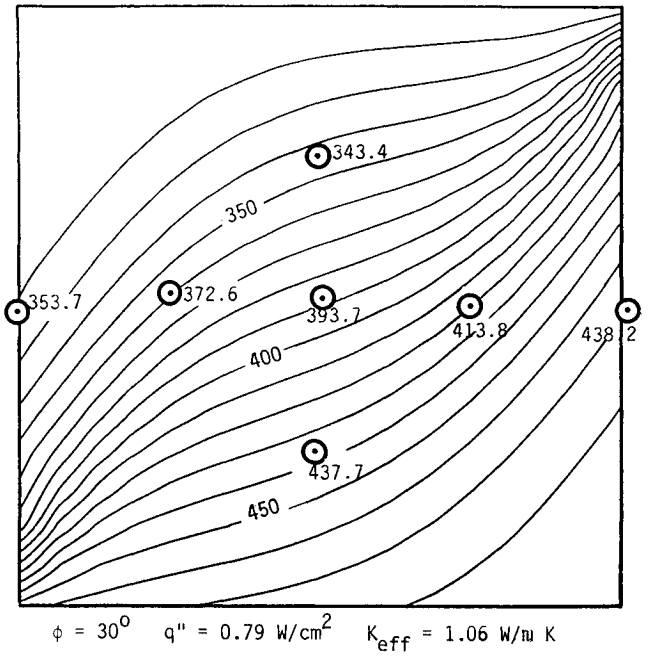

Fig. 8 Predicted two-dimensional temperature distribution.

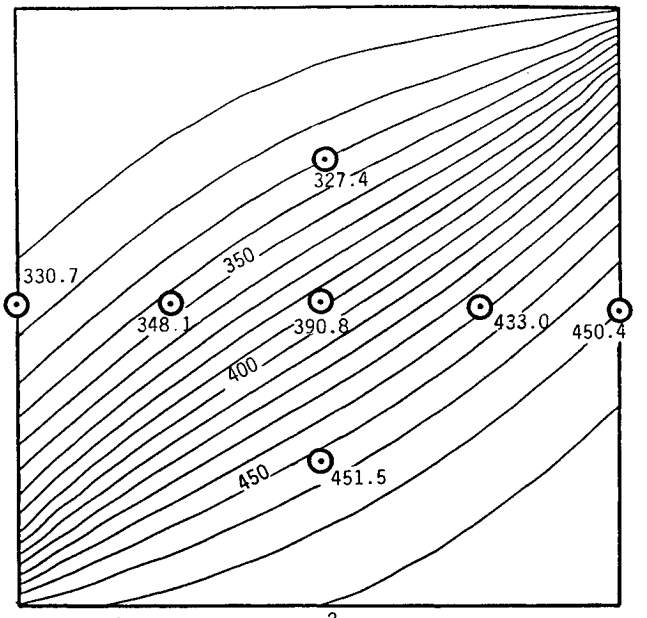

Fig. 9 Predicted two-dimensional temperature distribution.

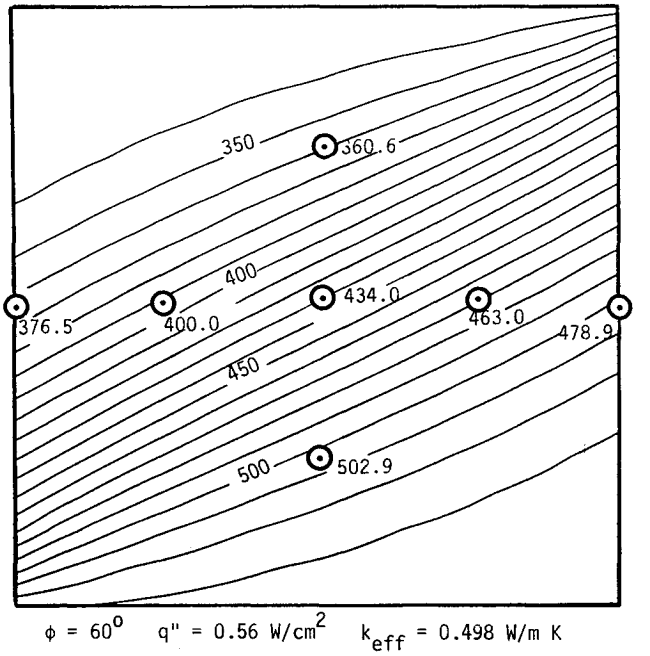

Fig. 10 Predicted two-dimensional temperature distribution.

the fiber angle on the dimensionless effective thermal conductivity, defined as the ratio of the effective thermal conductivity of the composite sample at the centerline to the thermal conductivity of the composite material in the fiber direction. As shown, the dimensionless thermal conductivity decreases with respect to fiber angle. This is to be expected since the thermal conductivity of the fibers is an order of magnitude greater than the thermal conductivity of the matrix.

The experimental uncertainty is comprised of several elements. First is the uncertainty associated with the location of the thermocouples and the assumed direction of the fibers with respect to the sample centerline. Second, and more significant, is the uncertainty associated with the difference in the thermal conductivity of the samples and the heat flux meter used (stainless steel). When the thermal conductivity of the heat flux meter is high compared to the sample, the uncertainty is greater than when the thermal conductivity of the heat flux meter is low. Because the same heat flux meter was used for all samples and the sample thermal conductivity varied significantly, the overall uncertainty varied for each sample. The error bars shown in Fig. 5 illustrate this point and identify the overall experimental uncertainty associated with a 90% confidence level for each sample tested.

Comparison of Numerical and Experimental Results

Using the measured thermal conductivity for the 0 deg specimen as k_l and the 90 deg specimen as k_m, the numerical model was used to predict the temperature distribution of the test samples. Prior to comparing this predicted temperature distribution with those obtained experimentally, an important difference should be noted. The assumption in the numerical model of a two-dimensional temperature distribution, assumption six, implies the sample is infinite in the third dimension. Because the sample is cylindrical, the dimension normal

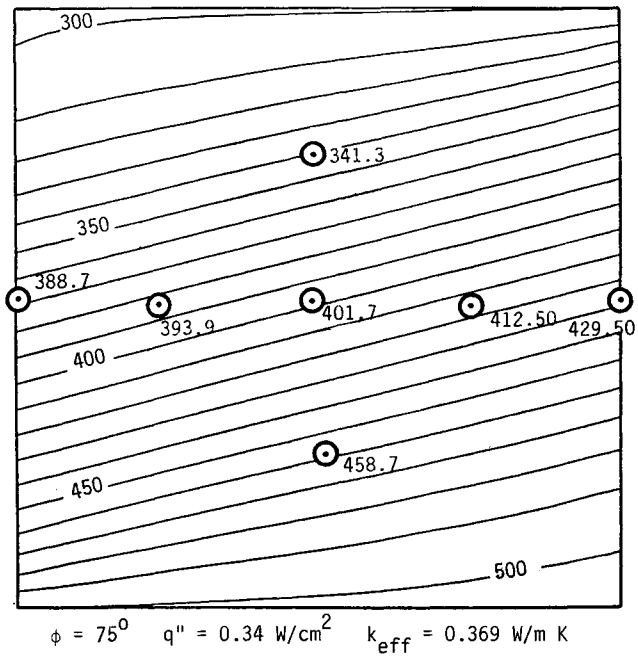

Fig. 11 Predicted two-dimensional temperature distribution.

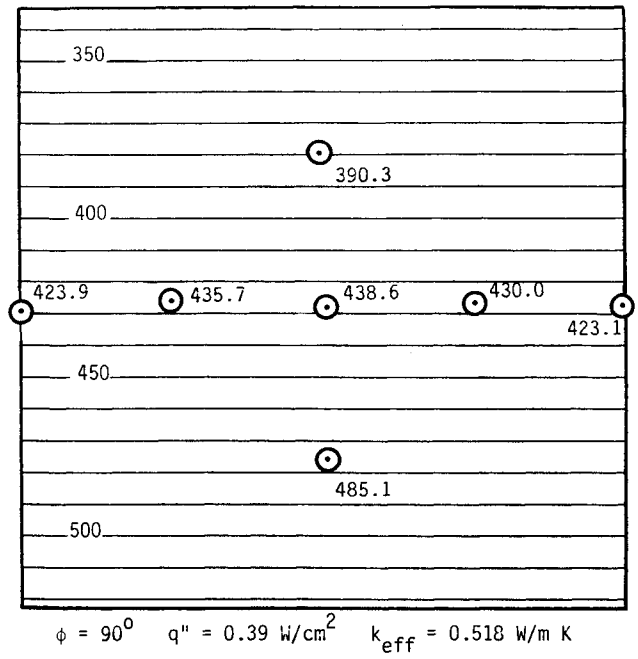

Fig. 12 Predicted two-dimensional temperature distribution.

to the plane being modeled is finite and crosses fibers. This causes a deviation in the temperature from what would be expected in an infinite sample, resulting in a reduction in the accuracy of the model.

Since the objective of the experimental portion of the investigation was to provide data for the verification of the numerical model, it is helpful to compare these results through the use of an overlay of the numerical predictions and the experimental data.

As shown in Figs. 6–12, when the experimental results are superimposed on the predicted values they show a good correlation between the data and the model. In Fig. 6, fiber angle = 15 deg, the predicted centerline temperatures agree with those measured experimentally quite well. Thermocouples *C* and *E* are within 7 K, and the surface thermocouples are within 20 K. This is not surprising since the further the thermocouple position from the centerline, the worse the approximation of two-dimensional temperature distribution.

In the 90 deg sample, Fig. 12, the variation in the measured thermocouple temperatures in the x direction indicates that this discrepancy between measurements and predictions in the higher fiber angle samples may be due to uncertainty in the thermocouple placement rather than shape effects of the cylindrical sample.

Conclusions

An experimental investigation utilized cylindrical samples to measure the effect of fiber direction on the temperature distribution and effective thermal conductivity of fibrous composite materials. Continuous unidirectionally aligned-fiber samples with PAN Type II fibers were chosen for the study because their thermal properties vary directionally but not with position as do the woven and random in-plane fiber composites. A numerical model was developed for predicting the two-dimensional heat conduction in aligned-fiber composite materials. The results of the experimental investigation were compared with the numerical model to determine the validity of the modeling technique.

In spite of the assumption of two-dimensional heat transfer in the numerical modeling, temperatures were within five to eight percent for all cases considered. As shown in the comparison of sample geometry and effective thermal conductivity, the samples with higher fiber angles were expected to fit the two-dimensional model closer than the low fiber angles, since the higher fiber angles are less sensitive to sample dimensions than the low fiber angle samples. This was found to be the case. The numerical model is verifiable within the experimental accuracy, although it should be applied only for two-dimensional cases as previously or in other configurations where the sample dimensions do not appear to affect the results.

Accurately predicting the edge effects requires a more sophisticated numerical model incorporating three-dimensional heat transfer. Additional experimental data are needed to verify this model, particularly in corner regions, where the edge effects dominate the heat transfer.

Acknowledgments

The authors would like to acknowledge the support of the Mechanical Engineering Division of the Texas Engineering Experiment Station for their support and also to thank the LTV Corporation, Dallas, Texas, for fabricating the experimental test specimens.

References

[1]Peterson, G. P. and Fletcher, L. S., "A Review of Thermal Conductivity in Composite Materials," AIAA Paper 87-1586, June 1987.

[2]Horvay, G., Mani, R., Veluswami, M. A., and Zinmeister, G. E., "Transient Heat Conduction in Laminated Composites," *Journal of Heat Transfer*, Vol. 95, Aug. 1973, pp. 309–316.

[3]Manaker, A. M. and Horvay, G., "Thermal Response in Laminated Composites," *Zeitschrift fuer Angewandte Mathematik und Mechanik*, Vol. 55, Sept. 1975, pp. 503–513.

[4]Hagen, K. D., "A Solution to Unsteady Conduction in Periodically Layered, Composite Media Using a Perturbation Method," *Journal of Heat Transfer*, Vol. 109, Nov. 1987, pp. 1021–1023.

[5]Hull, D., *An Introduction to Composite Materials*, Cambridge University, London, 1981, Chap. 1.

[6]Horvay, G. and Manaker, A. M., "Heat Flow in Laminated Composites Parallel to the Layering when the Surface Heating is of High Frequency," *Proceedings of the American Institute of Mining, Metallurgical, and Petroleum Engineers Conference on Composites*, Vol. 2, AIME, New York, 1975, p. 257.

[7]Kowalski, G. J. and Mitchell, J. W., "An Analytical and Experimental Investigation of the Heat Transfer Mechanisms within Fibrous Media," ASME Paper 79-WA-HT-40, Dec. 1979.

[8]Lee, H. J. and Taylor, R. E., "Thermal Diffusivity of Dispersed Composites," *Journal of Applied Physics*, Vol. 47, Jan. 1976, pp. 148–151.

[9]Maewal, A., Bache, T. C., and Hegemier, G. A., "A Continuum Model for Diffusion in Laminated Composite Media," *Journal of Heat Transfer*, Vol. 98, Feb. 1976, pp. 133–138.

[10]Schneider, G. E. and Romilly, D., "The Apparent Thermal Conductivity of Long Cylindrical Fibers in a Matrix," ASME Paper 79-WAM-HT-42, Dec. 1979.

[11]Han, L. S. and Cosner, A. A., "Effective Thermal Conductivities of Fibrous Composites," *Journal of Heat Transfer*, Vol. 103, May 1981, pp. 387–392.

[12]Behrens, E., "Thermal Conductivities of Composite Materials," *Journal of Composite Materials*, Vol. 2, No. 1, Jan. 1968, pp. 2–17.

[13]Ozisik, N. M., *Heat Conduction*, Wiley, New York, 1980, Chap. 15.

[14]Havis, C. R., "Effects of Fiber Direction on Heat Conduction in Unidirectionally Aligned Fiber Composites," M.S. Thesis, Mechanical Engineering Department, Texas A&M University, College Station, TX, 1987, pp. 1–41.

[15]Devore, J. L., *Probability and Statistics for Engineering and the Sciences*, Brooks and Cole, Monterey, CA, 1982.